PHILOSOPHICAL TRANSACTIONS OF THE ROYAL SOCIETY A MATHEMATICAL, PHYSICAL & ENGINEERING SCIENCES

Some Observations of Earth Strain Tides in California

J. Berger and F. Wyatt

Phil. Trans. R. Soc. Lond. A 1973 **274**, 267-277
doi: 10.1098/rsta.1973.0052

Phil. Trans. R. Soc. Lond. A. **274**, 267–277 (1973) [267]
Printed in Great Britain

Some observations of Earth strain tides in California

By J. Berger and F. Wyatt
Institute of Geophysics and Planetary Physics, University of California, San Diego, U.S.A.

A year of continuous strain data is analysed to reveal a secular strain rate of 1.6×10^{-7}/year north–south expansion superimposed on an apparent yearly cycle of 4×10^{-7} strain amplitude. Evidence is presented to show that thermoelastic effects are appreciable both at yearly and tidal periods. Three component strain tides are analysed to produce tidal phasors that indicate substantial discrepancies between the predicted Earth tide including a model coastal ocean tide and the observed strain tide. Further refinements on the ocean tide and the loading Green's function appear to be needed.

Introduction

The application of the laser to the field of geophysics has made great improvements in some of the existing instrumentation and provided a basis for some totally new instrumental concepts (Berger 1972). In the measurement of earth strain, lasers were quickly employed in interferometric strainmeters which could be quite long (Vali & Bostrom 1968; Berger & Lovberg 1969), and extremely stable (Levine & Hall 1972). Basically, these wide band instruments were designed to study the full spectrum of Earth strain phenomenon from long-term secular strain rates associated with seismo-tectonic activity to the suspected high-frequency gravitational radiation from pulsars (Levine & Stebbins 1972).

Studies of the Earth tides using strainmeters have been conducted by Ozawa (1952) and his co-workers in Japan, by Benioff (1959), Major, Sutton, Oliver & Metsger (1964), Berger (1970), Smith & Jungels (1970) in the United States and by King & Gerard (1969) in the United Kingdom. From the early work in Japan of Ozawa and the later observations of Kuo (1969) and Berger (1970) it became clear that the effects of the ocean tides loading the Earth's crust constituted an appreciable fraction of the observed strain tide signal at least for stations near the coast. The work of Farrell (1970, 1972) on the calculation of a surface-loading Green function for a radially structured spherical Earth, coupled with the advances made recently in successfully explaining the ocean-loading effect on gravimetric observations (Farrell 1970; Kuo, Jachons, Ewing & White 1970) have lent a new impetus to the study of the solid earth tides.

2. Instrument and site description

The instruments from which the observations were obtained are surface laser interferometric strain meters (l.s.m.) designed and developed over the past few years by the authors and Dr R. Lovberg at the University of California, San Diego. There are currently three instruments operating at two observatories, one near the campus in La Jolla and two at a remote mountain site to the east of Los Angeles.

The basic design of the instrument, described more fully elsewhere (Berger & Lovberg 1970), is illustrated in figure 1. The end piers, the fiducial points of the experiment, are columns of black granite set into holes drilled some 2 to 4 m into the ground. The piers are attached only along their lower $1\frac{1}{2}$ or 2 m with the rest of the hole filled by insulating material. This method

decouples the pier from the surface layers of the ground which undergo large diurnal temperature fluctuations and variations of moisture content.

The optical configuration is that of an unequal path Michelson interferometer with the light source, a He–Ne laser, and the local arm retroreflector sitting on one pier and the remote retroreflector on the other pier. The optical path between the two ends is contained in an evacuated tube 800 m long, suspended on a system of roller supports and tied to the ground only at its midpoint with the thermally induced length changes removed at each end by servo-controlled telescopic joints.

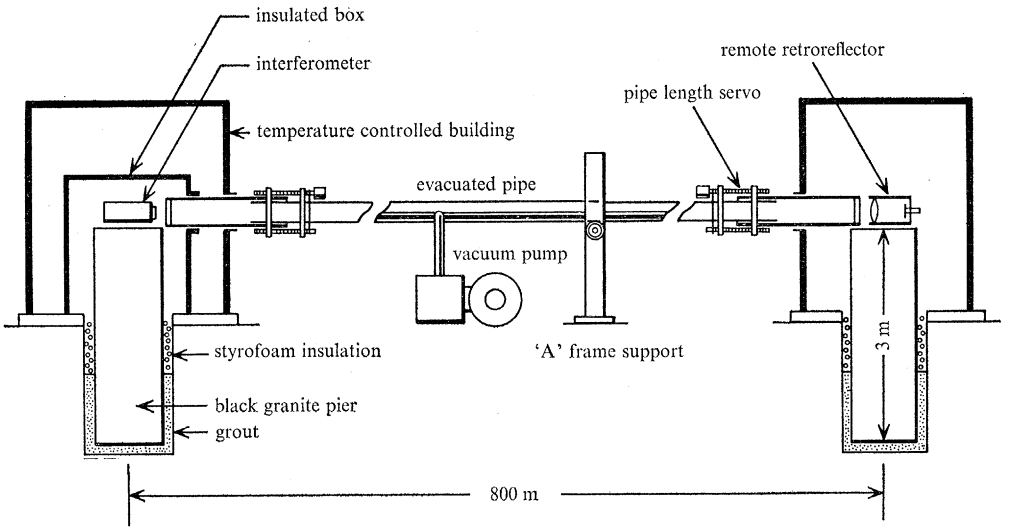

FIGURE 1. Mechanical design of laser strain meter.

In order to make interferometric measurements of earth strain with the stability necessary to study such phenomena as normal modes, earth tides and secular behaviour, it is imperative that some scheme of laser frequency stabilization by employed (Berger & Loveberg 1970; Levine & Hall 1972). The system we use locks the laser's frequency to the resonant frequency of a high Q optical resonator (a Fabry–Perot etalon), which is determined primarily by the length of a piece of fused quartz tube housed in a closely controlled environment. We estimate the stability of this system to be on the order of 10^{-9} a year.

The location and seismo-tectonic environment of the two field observatories is illustrated in figure 2. The dominant tectonic feature in Southern California is the San Andreas fault system which forms the boundary between the North American and Pacific plates. Relative motions of these two plates, on the average of some 5 cm/year, occur either as fault creep or as strain accumulation along the fault. Near San Bernardino, east of Los Angeles, the fault takes a bend from its predominant NW–SE orientation to an east–west trend. In the Imperial Valley, to the south of the Salton Sea, evidence indicates the existence of a small spreading centre (J. Brune, personal communication). Thus the predominant right lateral motion along the fault is broken in at least two places. At the spreading centre, a north–south spreading is consistent with right lateral motion on the fault. The east–west bend at San Bernardino, however, presents an obstruction to this right lateral motion. Here, the theory and geological observation indicate that the fault is locked and thrust motion occurs. Thus strain is likely to be accumulating in this region. Indeed, the area was probably loaded by some 10 m of potential displacement by the

1857 Fort Tejon earthquake. (Interestingly enough, the region to the north of San Bernardino where this magnitude 8.5 earthquake occurred has since been abnormally quiescent seismically.)

The Elliott Observatory (E.G.O.) was located not so much on the basis of geophysical interest as on considerations of proximity to the University as a proving ground for instrumental development. There is one l.s.m. at this site oriented NE–SW. The Piñon Flat Observatory

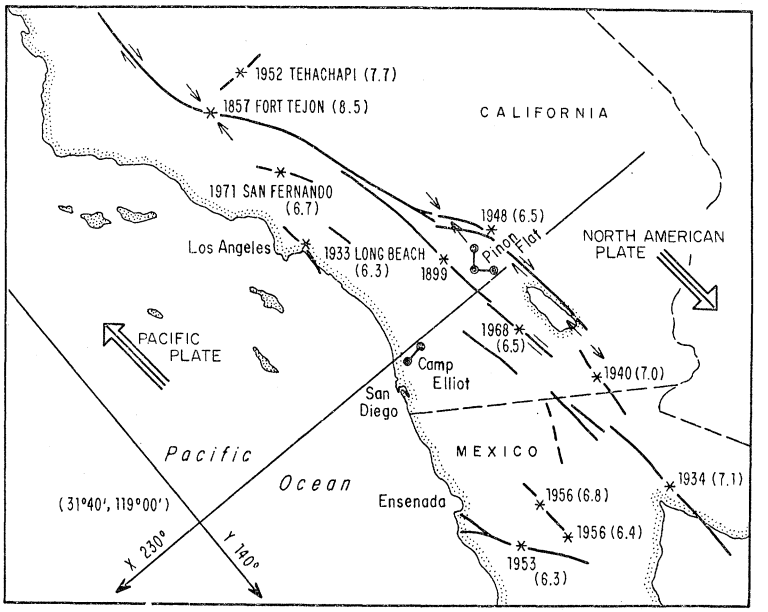

FIGURE 2. Site location map of laser strain meter observations and prominent tectonic features of Southern California. The coordinate system was chosen for analysis of ocean tides off the California coast.

(P.I.F.G.O.) was chosen to lie between the main trace of the San Andreas fault and the highly active San Jacinto fault. It is located in the wedge of granite that forms the San Jacinto Mountains in an area of suspected higher stress. Some pertinent information on these sites is summarized in table 1.

TABLE 1

station	lat.	long.	elevation	strainmeter orientation (true)	surface geology	other instrumentation
Elliott Geophysical Observatory E.G.O.	32.88°	117.1° W	200 m	N45° E	Caliche overlying pleistocene marine terrace deposits. Basement rocks of Franciscan formation at unknown depth	Block–Moore gravimeter. J–M seismometer. 3 component, 200 m liquid level tiltmeter. Microbarograph (nearby La Jolla labs have three component Press–Ewing seismometers)
Piñon Flat Geophysical Observatory P.I.F.G.O.	33.59°	116.46° W	1400 m	N0° E N90° E	decomposed granite grading into granitic bedrock 0 to 10 m below surface	La Coste tidal gravimeter. Two component Electrolevels tiltmeters. Two component Hughes tiltmeters. Microbarograph. Thermograph. Two ground thermographs

3. Data recording and reduction

The data recording system is depicted schematically in figure 3. The fringe counters have two outputs, one at a sensitivity of one count per fringe or a least count strain of 4.3×10^{-10} and the other at a sensitivity of $\frac{1}{4}$ of this or 10^{-10} strain. This latter must be filtered before recording at one sample per record to prevent aliasing by high frequency noise (whose amplitude occasionally is 2×10^{-10}).

The outputs from the fringe counters are recorded by three independent systems partly to separate the higher frequency seismic data from the tidal and secular data and partly to provide some redundancy in the recording system so that total failure will be extremely rare.

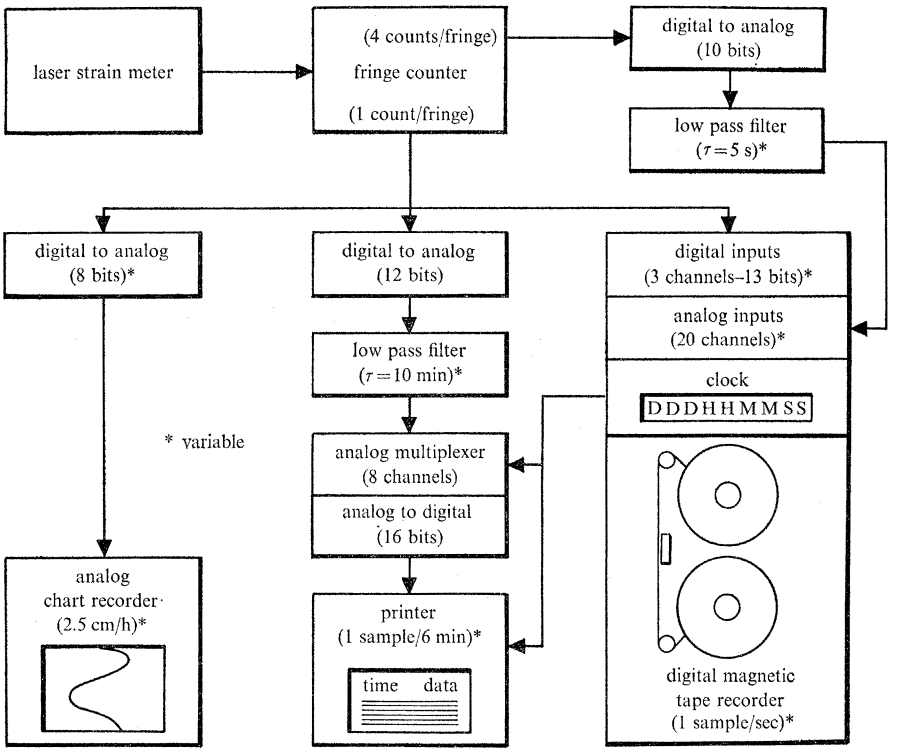

Figure 3. Diagram of main data recording system.

The primary recording medium is digital magnetic tape where the strain data, sampled once per second, are recorded along with the outputs of various other instrumentation at the observatory. The digital input from the full fringe counter is augmented with a filtered version of the quarter fringe data.

In the analysis of long periods of data (weeks and longer) reducing 1 s data on a computer is cumbersome and expensive and so a hard-copy data logging system which employs a digital printer samples the output of a low-passed signal once every 6 min. The printer paper is the prime source of data for tidal and secular studies. In case of failure, however, this data can be recovered from either the magnetic tape or from a strip chart recording that runs at 2.5 cm/h.

The data from the digital printer are punched on cards, edited (for the removal of offsets and spikes) and stored on magnetic tape and in card format at the 6 min interval. For secular and

long-term studies, the data are low-pass filtered to remove frequencies above $\frac{1}{5}$ c/h. For the tidal analysis reported here, the data are band-pass filtered to remove all frequencies outside the band $\frac{1}{40} \leqslant f \leqslant \frac{1}{5}$ c/h and decimated to a sample rate of once per hour.

4. Results

(a) *Secular strain*

Figure 4 shows the total secular strain record for the north–south component at P.I.F.G.O. The ground temperature sensed at a depth of $\frac{1}{2}$ and 1 m is also plotted for a somewhat shorter time interval. (Air temperature and air pressure are also routinely recorded.)

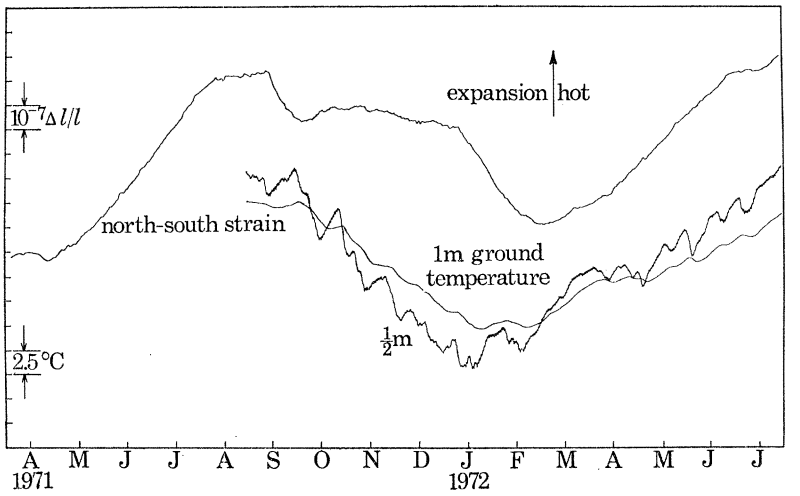

Figure 4. North–south secular strain and ground temperature records from P.I.F.G.O. for period of 17 March 1971 to 15 July 1972. The strain data has been filtered to remove all frequencies above 0.6 c/day.

What appears to be an annual cycle with a strain amplitude of 4×10^{-7} is the dominant feature of the record. The phase lag of this apparent strain cycle behind the air temperature cycle is some 60° (corresponding to a time delay of 2 months) which argues strongly against a direct instrumental effect causing the strain cycle. The ground temperature at 1 m also displays an annual cycle of some $6\frac{1}{2}$ °C amplitude but its phase leads the phase of the ground strain by some 20°. From a knowledge of the temperature at $\frac{1}{2}$ and 1 m depth it is estimated that at a depth of $1\frac{1}{2}$ m the ground temperature is in phase with the strain and has a yearly amplitude of some $5\frac{1}{2}$ °C.

Thermoelastic stresses will be produced by spatial and temporal temperature variations on the ground surface. Even though the temperature field falls off very rapidly with depth, the induced stresses are felt to a depth determined by the horizontal extent of the temperature variations and so the vertical wavelengths of these stresses are the horizontal wavelengths of the driving temperature disturbances. At a frequency of a cycle per year, the horizontal wavelength must be of the order of 10^2 km. The upper limit is set by the distance from the site to the constant temperature bath of the ocean (120 km for Piñon Flat) and much shorter wavelength temperature variations are averaged out over this period. Thus, for thermoelasticity induced strains, the fiducial points of the strainmeter are essentially at the surface and there should be no appreciable phase lag between temperature and induced strain. This implies that if the observed strain is to

be explained by thermoelastic stress, the thermal input is not at the surface, but at a depth of some $1\frac{1}{2}$ m, the material above acting as an insulator incapable of transmitting much stress. The possibility cannot be eliminated at this time, however, that part of the observed strain record might be produced by pier tilt in response to temperature fluctuations at its base. To produce the observed annual cycle a tilt of 2×10^{-4} rad would be necessary which, if it occurred on the instrument pier, would produce a 16 cm displacement of the laser beam at the far end. Although this amount of tilt is unlikely, tiltmeters have been installed on the piers to investigate the magnitude of the effect.

The observed secular strain rate during this period was approximately 1.6×10^{-7}/year in the sense of north–south expansion. Some of this could also be the result of pier tilt but it is worth noting that this figure is an order of magnitude lower than the value usually quoted for California (Benioff 1959).

TABLE 2. RESULTS OF 7867 h (0.898 YEAR) FOURIER ANALYSIS OF BAND PASSED OBSERVATIONS ($\frac{1}{40}$ TO $\frac{1}{5}$ c/h)

				observations	
tidal line	frequency c/day	period h	theoretical amplitude $\times 10^{-9}$	δ	$\Delta\phi$
Q_1	0.894	26.84	0.722	0.766	6.8°
O_1	0.930	25.81	4.51	0.930	−14.2°
M_1	0.966	24.84	0.440	0.909	69.4°
P_1	0.997	24.07	0.910	2.31	69.3°
S_1	1.000	24.00	2.08	2.95	−7.4°
K_1	1.003	23.95	6.01	0.718	−23.5°
J_1	1.039	23.12	0.232	1.97	−41.7°
$2N_2$	1.860	12.90	0.385	1.33	−18.9°
N_2	1.896	12.66	2.41	0.888	8.4°
M_2	1.932	12.42	13.3	0.823	−3.4°
S_2	2.000	12.00	5.05	0.763	3.9°
K_2	2.007	11.96	2.14	1.08	7.3°

(*b*) *The tidal strain spectrum*

Table 2 gives the results of the Fourier analysis of slightly under one year (7867 h) of strain data from the Piñon N.S. instrument. We have restricted our attention to the frequency band between $\frac{1}{40}$ and $\frac{1}{5}$ c/h. The theoretical amplitudes were calculated by identical analysis of the theoretical strain tides (Berger 1970).

The lines which have been identified unambiguously all have amplitudes greater than 2×10^{-10}. Unfortunately, the noise level seems to preclude positive identification of lines with smaller amplitudes at least with this amount of data. Even with 7865 h of data the P_1, S_1 and K_1 lines are barely resolved.

There seems to be some thermal contamination of the strain record. Evidence for this may be seen in figure 5 in the anomalous S_3 peak (peaks at multiples of the solar period can be identified up to the fifth harmonic) and in the large amplitude of the S_1 component (see table 2).

The results of the spectral analysis of the air temperature at Piñon Flat for this period reveal fairly broad peaks at the solar period at its harmonics. At 1 c/day the peak is broad enough to cause contamination of the P_1 and K_1 strain peaks as well as the S_1. Further, there is evidence of the familiar cusping in the region of the main spectral peaks (Munk & Cartwright 1966).

There are two ways that the strain record could be temperature sensitive. First, there could

be an instrumental temperature coefficient in the interferometer itself or in the instrument-ground interface. We have performed a series of tests on the interferometer itself which gives us confidence that the various parts of the apparatus do not have large enough coefficients to explain the observed strain anomalies.

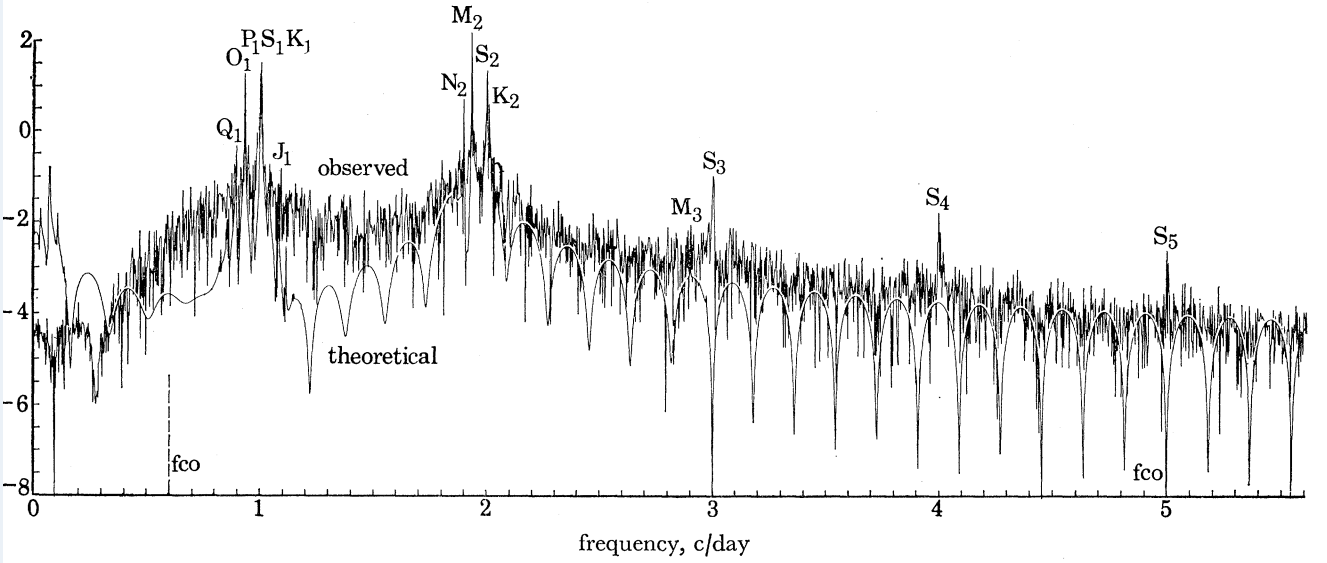

FIGURE 5. Spectrum from one year of north–south strain compared with corresponding spectrum of theoretical strain. The observed strain was band-pass filtered to include only those frequencies between 0.6 and 5 c/day.

The second method by which contamination of the strain record can be caused is by the direct thermoelastic effect on the earth's surface as discussed above. The amplitude at this site of the average day to night temperature fluctuations is about 10 °C, but the horizontal wavelength is difficult to measure since it will be influenced by topography and surface albedo. If one models the problem as a sinusoidal temperature variation on a homogeneous halfspace, a 20 km wavelength is necessary, with the measured diurnal temperature fluctuation, to produce an effect whose magnitude is 2.5×10^{-9} (some 50 % of the observed S_1 strain amplitude). This seems like a reasonable figure when one considers that at this site, within 20 km the elevation varies between sea level at the desert floor and 3000 m at a mountain top.

(*c*) *Three component strain tides*

To provide some further insight into the discrepancies between the theoretical and observed earth tides, one month of data recorded simultaneously on the north–south and east–west instruments at P.I.F.G.O. and on the NE–SW instrument at E.G.O. were analysed (see figure 6). The results are given in table 3. For simplicity, all amplitudes are normalized to the theoretical north–south amplitude and the phases referred to the phase of the geopotential at P.I.F.G.O. E.G.O. being some 0.6° farther west in longitude has a 0.6° and 1.2° phase lag for the diurnal and semidiurnal species respectively.

There are not enough data to resolve the $P_1S_1K_1$ triplet or the S_2K_2 lines and hence, because of the apparent temperature effect evident in the years' record, these lines are considered unreliable. The O_1 and M_2 lines, however, show a great deal of consistency when analysed over different time periods and they have the additional advantage that they are of relatively large

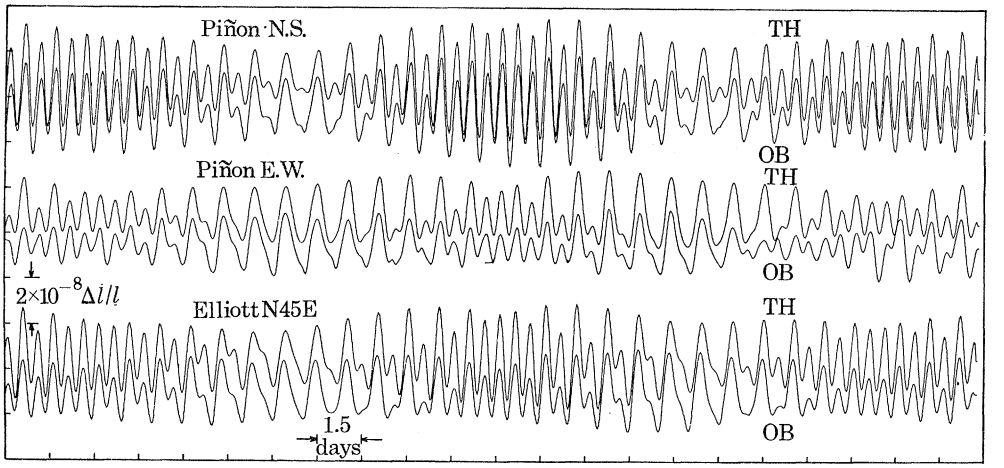

FIGURE 6. Three components of simultaneously observed strain and the respective theoretical strains from 26 February to 29 March 1972. The observed records have been band-pass filtered to include only those frequencies between 0.6 and 5 c/day.

TABLE 3. RESULTS OF THE SPECTRAL ANALYSIS OF THREE COMPONENT TIDES

The letter T refers to the theoretical tide, O to the observed and D to the difference vector between the theoretical and the observed (see figures 7 and 8).

	M_2		O_1	
line	amplitude relative to T_N	phase relative to Piñon potential	amplitude relative to T_N	phase relative to Piñon potential
T_N	1.000	0.0°	1.00	0.0°
T_{45}	0.756	18.2°	1.36	−22.9°
T_E	0.399	0.0°	1.55	0.0°
O_N	0.829	0.9°	0.775	9.4°
O_{45}	0.519	31.7°	1.49	−0.9°
O_E	0.358	20.6°	1.54	−18.2°
Elliott pot.	—	−1.2°	—	−0.6°
D_N	0.167	175.6°	0.269	151.5°
D_{45}	0.278	166.3°	0.559	70.2°
D_E	0.141	116.4°	0.489	−100.5°

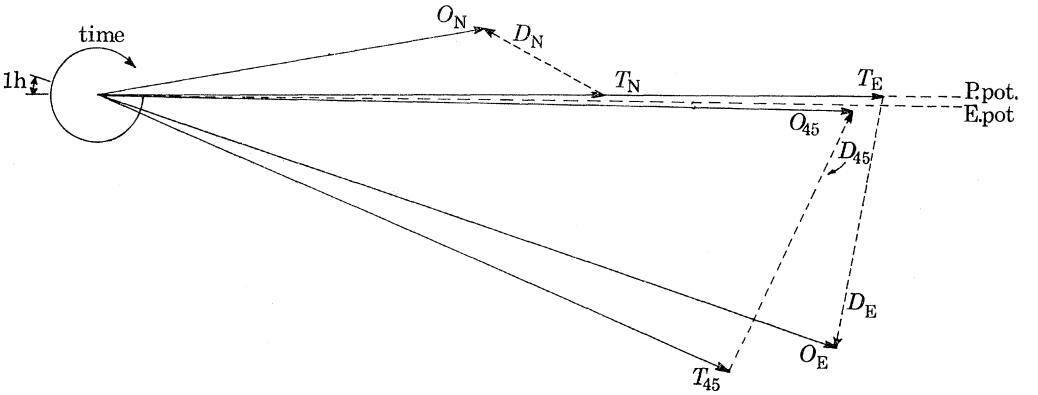

FIGURE 7. O_1 tidal phasor, indicating observed (O) amplitudes and phases relative to theoretical (T) amplitudes and phases for the 0.930 c/day line of the strain spectra. All vectors have been normalized to the Piñon north–south theoretical strain amplitude and geopotential phase. Subscript N refers to Piñon north–south strainmeter, E refers to Piñon east–west strainmeter, and 45 refers to Elliott northeast–southwest strainmeter. D denotes the difference vector.

amplitude. The phasor diagrams for the O_1 and M_2 lines are shown in figures 7 and 8. It is evident that the difference vectors amount to a substantial fraction of the theoretical. Moreover, at these frequencies, there would not seem to be any large noise sources besides the ocean tidal loading.

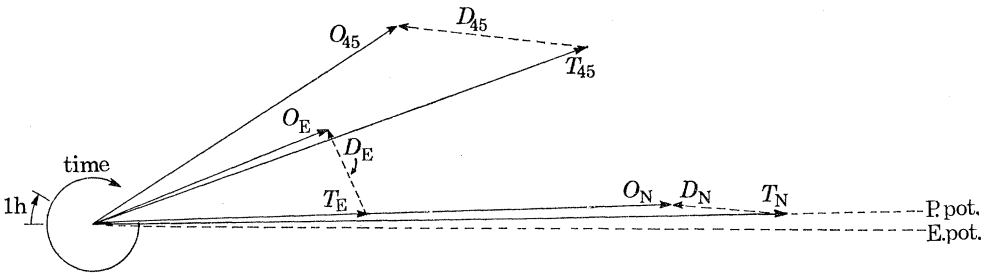

FIGURE 8. M_2 tidal phasor, indicating observed amplitudes and phases relative to theoretical for the 1.932 c/day line of the strain spectra.

The ocean tide along the California coast has been thoroughly investigated (Munk, Snodgrass & Wimbush 1970). The observed semidiurnal tide fits nicely a model that consists of a wave, trigonometric along the shore and exponential offshore, which travels up the coast from SE to NW. The general form of the tide source is given by Munk *et al.* (1970) as

$$\eta = \eta_0 \exp\{\mathrm{i}(\alpha x + \beta y - \omega t - \psi)\} \quad \text{for} \quad x < 0.$$

(See figure 2 for the coordinate system.)

For the M_2 tide the dominant component has the parameters $\eta_0 = 49$ cm, $\alpha = -\mathrm{i}/2170$ km^{-1}, $\beta = -1/1270$ km^{-1}, $\psi = 88°$ referred to the equilibrium potential at Piñon Flat.

It has been shown by Berger (1970) that a load of this form on an infinite elastic halfspace will produce a strain given by

$$e(x, y)_{z=0} = \frac{\eta_0}{4(\lambda+\mu)} \left[\frac{|\beta|}{|\beta| - \mathrm{i}\alpha}\right] \exp\{|\beta|\, x\} \exp\{\mathrm{i}(\beta y - \omega t - \psi \pm 2\theta)\},$$

where λ and μ are the Lamé parameters and where θ, the angle between the strainmeter and the x-axis, has its sign chosen to agree with the sign of β. So, for example, the M_2 tide which propagates northward upshore (in the negative y-direction) has $\beta < 0$ and so negative sign is chosen. The phase lead of the theoretical strain correction vector, relative to the Piñon geopotential is

$$\phi = \psi + 2\theta + |\beta| y.$$

The phase angles for the various components are given in table 4.

TABLE 4. OCEAN LOAD VECTORS

strainmeter	θ	y/km	ϕ
Piñon north–south	50°	−18.0	189°
Piñon east–west	−40°	−18.0	49°
Elliott N45° E	5°	+7.5	94°

These values may be compared with the phase angles of the difference vectors shown in the M_2 tidal phasor (figure 8). While the phase angles of these vectors are sensitive functions of the phase angles and amplitudes of the observed vectors, only the north–south difference vector D_N is close to agreeing with the theory.

It has been suggested (Ozawa 1957; Kuo 1969) that the areal strain e_A given by

$$e_A = e_{\theta\theta} + e_{\lambda\lambda}$$

should be less sensitive to ocean loading then either of the two components. We find, however, that the areal strain is in no better agreement with the theory than the north–south component. The results are quite similar; the observed areal strain is some 22 and 19 % too small with phase angles of 2.7 and $-11.3°$ for the M_2 and O_1 components respectively. Indeed, an examination of the theoretical results of Farrell (1972) who calculated an areal strain Green function for a realistic spherical Earth model, shows an areal strain produced by surface loading which can be as much as 50 % of the linear strain calculated for the same load on a homogeneous halfspace.

The ocean tidal model of Munk *et al.* (1970) was designed to fit only the Pacific coastal tides and does not include the effects of the Gulf of California or the effects of offshore tides. These corrections are currently being investigated and the loading Green function of Farrell (1972) will be used to perform a convolution with the co-tidal charts to produce the strain on a radially structured Earth.

5. Summary

The analysis of a year's observations at Piñon Flat Observatory indicated a secular strain rate less than 1.6×10^{-7}/year in the sense of north–south expansion superimposed by an apparent annual cycle of 4×10^{-7} amplitude. Observations of ground temperature at two depths showed that at a depth of $1\frac{1}{2}$ m the annual temperature cycle was in phase with the observed strain cycle and has an amplitude of $5\frac{1}{2}$ °C. This implies that the strain cycle is probably due to thermoelastic stresses induced below a loose insulating layer of decomposed granite, although temperature-induced pier tilt cannot definitely be ruled out as a partial source at this time.

The spectral analysis of the year's tidal record revealed peaks at all frequencies where the theoretical strain amplitude was greater than 2×10^{-10}. Further evidence for thermoelastic strain was seen in the anomalous spectral amplitudes at a cycle per solar day and its harmonics. It is argued that the implied horizontal wavelength of the temperature disturbances is reasonable in the light of local topography, although considerable uncertainty is involved in the calculations of both the thermal and elastic behaviour due to the unconsolidated nature of the surface material and our lack of knowledge of the correct elastic and thermal parameters.

A month of three component tides (north–south, east–west and NE–SW) were analysed to produce tidal phasor diagrams at the O_1 and M_2 tidal peaks. The M_2 phasor was compared with the ocean-loading effects produced by an ocean tidal model revealing some major discrepancies. Areal strain did not seem to give any better results than the best component strain. Further refinements to the ocean tide model such as the inclusion of the tides in the Gulf of California and the incorporation of a more realistic earth model are currently in progress.

The authors wish to thank Professor R. H. Lovberg for his consultations on instrumental matters, Professor R. L. Parker for his assistance on data reduction and computing problems, Professors W. H. Munk and R. A. Haubrich for their helpful discussions on ocean and Earth tides and to Mr Leo Wueve for his admirable assistance in the field. This work was supported by the National Oceanic and Atmospheric Administration under Grant N22-17-72(G) and by the National Science Foundation under Grant GA-25700. The land for P.I.F.G.O. was made available through the kind cooperation of the United States Forest Service, San Bernardino National Forest.

PHILOSOPHICAL TRANSACTIONS OF THE ROYAL SOCIETY A MATHEMATICAL, PHYSICAL & ENGINEERING SCIENCES

References (Berger & Wyatt)

Benioff, H. 1959 *Bull. geol. Soc. Am.* **70**, 1019–1032.
Berger, J. 1970 Ph.D. Dissertation, University of California, San Diego.
Berger, J. 1972 *Adv. Geophys.* **14** (in the Press).
Berger, J. & Lovberg, H. R. 1969 *Rev. Scient. Instrum* **40**, 1569–1575.
Farrell, W. E. 1970 Ph.D. Dissertation, University of California, San Diego.
Farrell, W. E. 1972 *Rev. Geophys.* **10**, 761–797.
King, G. C. P. & Gerard, V. B. 1969 *Geophys. J. R. astr. Soc.* **18**, 437–440.
Kuo, J. T. 1969 *J. geophys. Res.* **74**, 1635–1643.
Kuo, J. T., Jachens, R. C., Ewing, M. & White, G. 1970 *Science, N.Y.* **168**, 968–971.
Levine, J. & Hall, J. L. 1972 *J. geophys. Res.* **77**, 2595–2607.
Levine, J. & Stebbins. 1972 *Phys. Rev.* D. **5**, 1465–1468.
Major, W., Sutton, G. H., Oliver, J. & Metsger, R. 1964 *Bull. seism. Soc. Am.* **54**, 295–346.
Munk, W. H. & Cartwright, D. E. 1966 *Phil. Trans. R. Soc. Lond.* A **259**, 533–581.
Munk, W. H., Snodgrass, F. & Wimbush, M. 1970 *Geophys. Fluid Dynamics* **1**, 161–235.
Ozawa, I. 1952 *Diaster Prevention Res. Inst., Kyoto University Bull.* **3**, 4–17.
Ozawa, I. 1957 *Diaster Prevention Res. Inst., Kyoto University Bull.* **15**.
Smith, S. W. & Jungels, P. 1970 *Phys. Earth Planet. Interiors* **2**, 232–238.
Vali, V. & Bostrom, R. C. 1968 *Rev. scient. Instrum.* **39**, 1304–1306.

PHILOSOPHICAL TRANSACTIONS OF THE ROYAL SOCIETY A MATHEMATICAL, PHYSICAL & ENGINEERING SCIENCES